Calculations on the Auger spectra of clusters modeling polymer chains

C.-M. Liegener and E. Weiss
Chair for Theoretical Chemistry, University Erlangen-Nürnberg, Egerlandstrasse 3, D-8520 Erlangen, Federal Republic of Germany

(Received 30 October 1989; revised manuscript received 9 February 1990)

Auger spectra of clusters modeling polyacetylene and polyethylene chains were calculated by an *ab initio* Green's-function method. Convergence of the line shape with increasing cluster size was reached with C_6H_8 and C_6H_{14}, respectively. In the polyacetylene sequence some gaps which are visible in the ethylene spectrum disappear almost completely for larger clusters while a feature due to delocalization emerges at low binding energies. In the polyethylene sequence a three-peak structure similar to that of methane can be identified in the spectra of the larger clusters.

I. INTRODUCTION

Auger spectra of small molecules have the property that they reflect the local chemical environment of an atom as part of the molecular system.[1] This is due to the localization of the initial-state core hole, determining the transition rates in a way characteristic for the valence-electron density at the primary core ionization site. It is interesting to follow the changes of Auger spectra when gradually moving from small to larger systems. In the case of clusters modeling polymer chains the limit will be that of having the bulk states of an infinite system. Because of the local-probe character of Auger spectroscopy, one can expect that the bulk limit will be reached already using clusters of reasonably limited size. This has been experimentally confirmed for the Auger spectra of linear alkanes[2] approaching with increasing chain length the Auger spectrum of polyethylene.[3-5] Semiempirical calculations have been performed for the Auger spectra of linear alkanes and polyethylene.[2,6,7] *Ab initio* calculations have been reported only for the first member of the alkane series, methane.[8-14] We report here first *ab initio* calculations on C_nH_{2n+2} clusters with $n=1,\ldots,6$.

No studies have been performed for linear polyenes approaching polyacetylene in the infinite-chain limit, except for the first member of the series, i.e., ethylene, for which both semiempirical[11,15] and *ab initio* calculations[16] have been performed. Furthermore, the Auger spectrum of benzene, which may be interesting for comparison, has been studied by *ab initio* calculations.[17] The experimental spectra of ethylene and benzene have also been reported.[1,18,19] In the work presented here we have studied $C_{2n}H_{2n+2}$ clusters with $n=1,\ldots,3$ by means of *ab initio* Green's-function calculations.

II. METHOD OF CALCULATION

On the *ab initio* level there are essentially two approaches which have been applied to Auger spectra of molecules and clusters, namely wave-function methods (Refs. 20, 21, and references therein) and methods based on many-body perturbation theory (Green's-function methods[16,22,23] and the coupled-cluster method[24]). In the present work a version of the *ab initio* Green's-function method will be used, which is appropriate for obtaining qualitative results for larger clusters.[25]

The energetic positions of the Auger lines are given by

$$E_{\rm kin}=U_{\rm IP}^{(c)}-U_{\rm DIP}^{(v)}\ , \tag{1}$$

where $E_{\rm kin}$ is the kinetic energy of the Auger electron, $U_{\rm IP}^{(c)}$ is the core ionization potential (in Koopmans's approximation, $U_{\rm IP}^{(c)}=-\varepsilon_c$, where ε_c is the core orbital energy), and $U_{\rm DIP}^{(v)}$ is the double-ionization potential (DIP) for the final state of the transition.

The particle-particle Green's function has poles at $-U_{\rm DIP}$, which are calculated as zeros of the eigenvalues of the inverse particle-particle Green's-function matrix;

$$\underline{G}^{-1}(\omega)=\underline{G}^{(0)^{-1}}(\omega)-\underline{K}\ , \tag{2}$$

where $\underline{G}^{(0)}$ and $\underline{K}$ will be defined as follows. The first-order irreducible vertex part $\underline{K}$ is given by

$$\begin{aligned} K_{klmn}^{(S,T)}&=V_{klmn}+V_{klnm} \quad \text{if } k<l \text{ and } m<n\ ,\\ K_{klmn}^{(S)}&=V_{klmn} \quad \text{if } k=l \text{ and } m=n\ ,\\ K_{klmn}^{(S)}&=2^{1/2}V_{klmn} \quad \text{if either } k=l \text{ or } m=n\ , \end{aligned} \tag{3}$$

where V_{klmn} are the two-electron integrals, the indices refer to spatial orbitals, and the superscript refers to singlets (S) and/or triplets (T). Furthermore,

$$G_{klmn}^{(0)}(\omega)=\gamma_{kl}\delta_{km}\delta_{ln}/(\omega-\varepsilon_k-\varepsilon_l)\ , \tag{4}$$

where $\gamma_{kl}=-1$ if both indices k,l belong to occupied, $+1$ if both k,l belong to unoccupied orbitals, 0 otherwise, and $\varepsilon_k,\varepsilon_l$ are the valence orbital energies.

The transition rate R to a singlet S or triplet T final state is estimated as

$$R_v^{(S,T)}\sim d^{(S,T)}\sum_{l,m}\sum_{i,j,i',j'}M_{ij}^{(S,T)}(\phi_{lm})^{*}M_{i'j'}^{(S,T)}(\phi_{lm})\times \operatorname*{Res}_{-U_{\rm DIP}^{(v)}}(-G_{iji'j'}^{(S,T)})\ , \tag{5}$$

where $d^{(S)}=1$, $d^{(T)}=3$, and $M_{ij}^{(S,T)}$ is the matrix element of the electronic Hamiltonian between Hartree-Fock

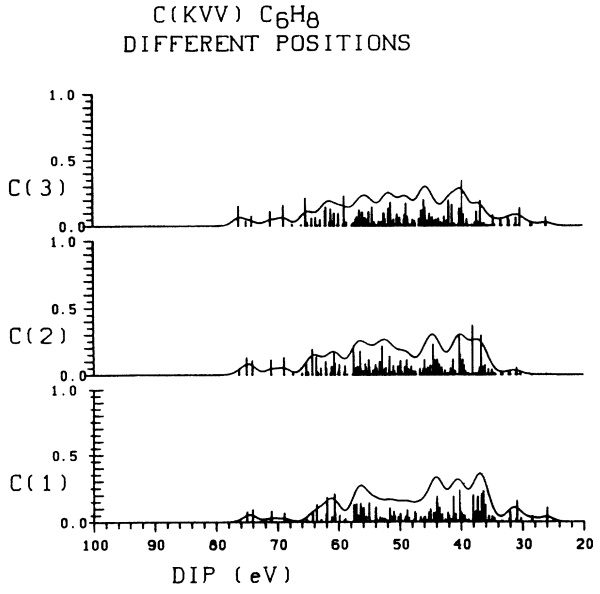

FIG. 1. Carbon Auger spectra for different atoms in C_6H_8. Atoms numbered subsequently from end to middle cluster positions.

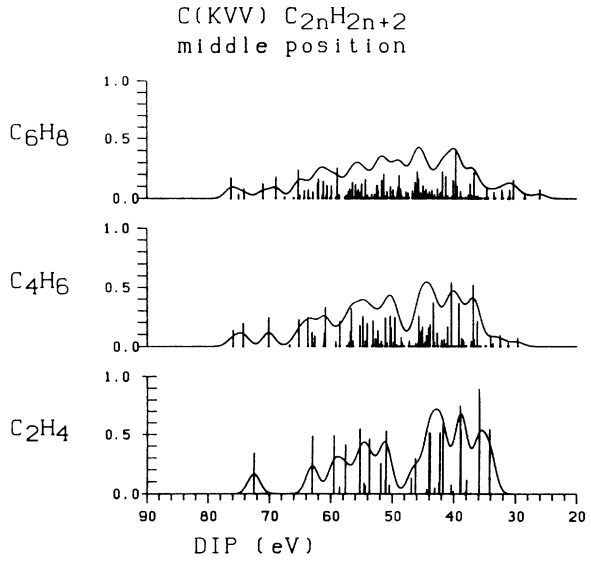

FIG. 3. Middle carbon Auger spectra for different clusters of the polyacetylene sequence.

states where the initial state has a core hole and the final state has holes in orbitals ϕ_i, ϕ_j, and an additional electron in a spherical continuum orbital ϕ_{lm} centered at the primary ionization site. These matrix elements are evaluated in the one-center model[26,27] by employing the radial integrals of McGuire.[28]

The Hartree-Fock data used in setting up the matrix-valued function $\underline{G}(\omega)$ were obtained with Clementi's $7s3p$-$2s1p$ and $4s$-$1s$ basis sets[29] using experimental poly-

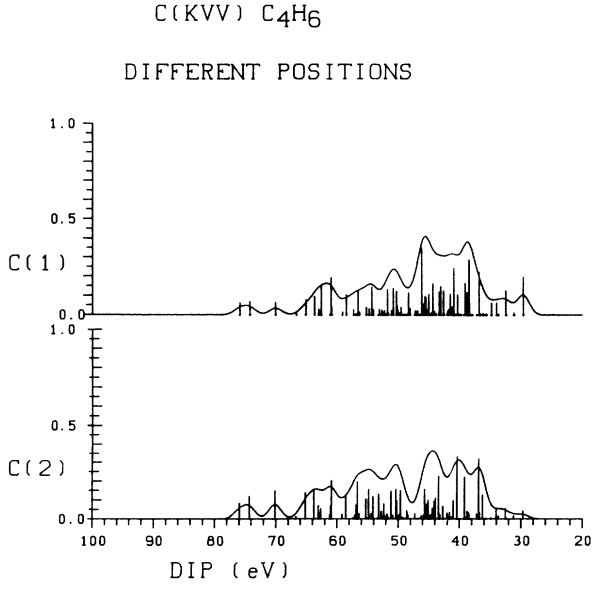

FIG. 2. Carbon Auger spectra for different atoms in C_4H_6. Atoms numbered subsequently from end to middle cluster positions.

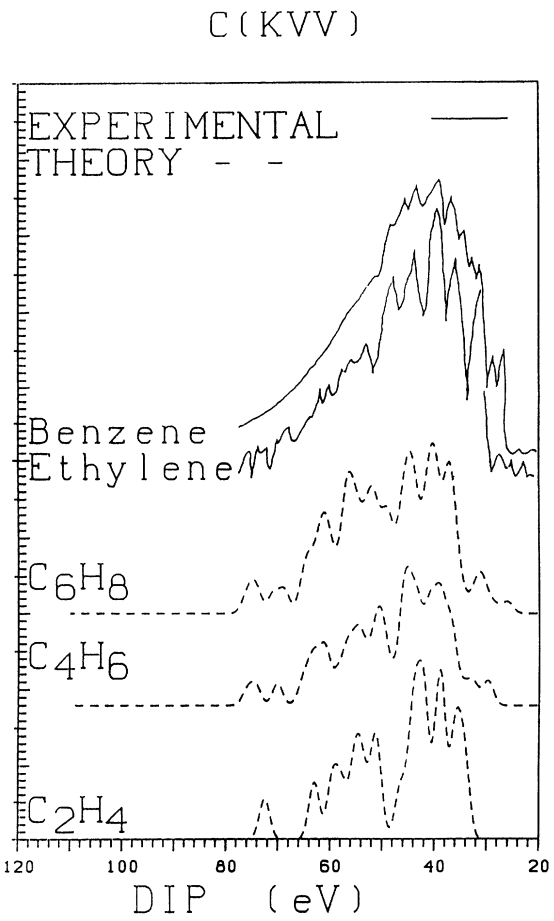

FIG. 4. Comparison of the resulting cluster Auger spectra of the polyacetylene sequence with the experimental Auger spectra of benzene and ethylene from Ref. 19.

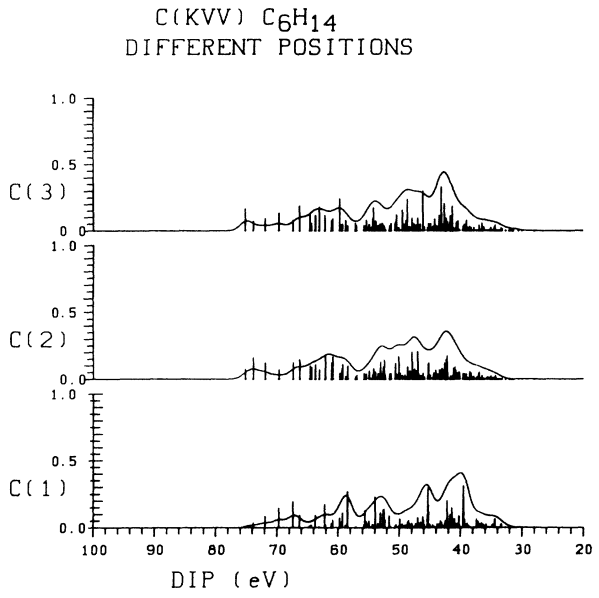

FIG. 5. Carbon Auger spectra for different atoms in C_6H_{14}. Atoms numbered subsequently from end to middle cluster positions.

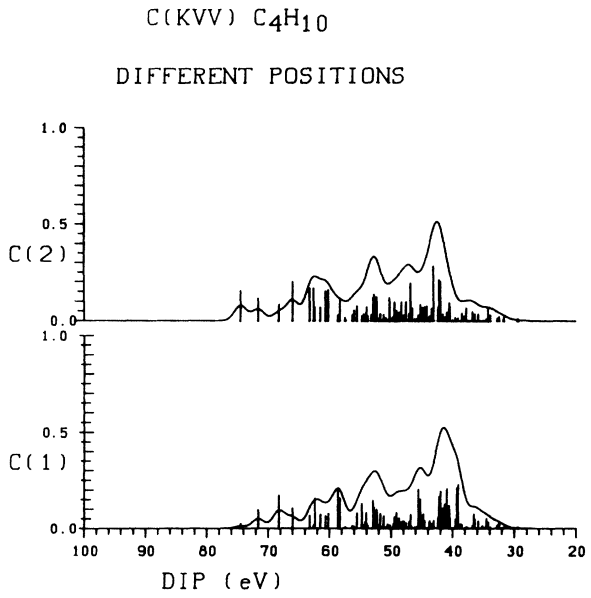

FIG. 7. Carbon Auger spectra for different atoms in C_4H_{10}. Atoms numbered subsequently from end to middle cluster positions.

mer distances for the geometries[30] and saturating the ends with hydrogen atoms. The lines obtained from Eqs. (1) and (5) were convoluted with Gaussians of appropriate widths to give the overall line shape. The widths have been determined (one for each spectrum) by comparison of the monomer spectra with experiment[1] and they have been kept constant throughout each sequence. This approach is deliberately chosen to simplify comparison of the spectra in a sequence.

In contrast to semiempirical approaches and more detailed studies of individual molecules we will not attempt in our model to study a perfect reproduction of experimental line shapes. For that purpose several adjustable widths for each spectrum should be used, consideration of satellite lines would be advisable[31] and further effects of electron correlation could be accounted for by scaling the transition matrix elements.[32] Furthermore, basis-set

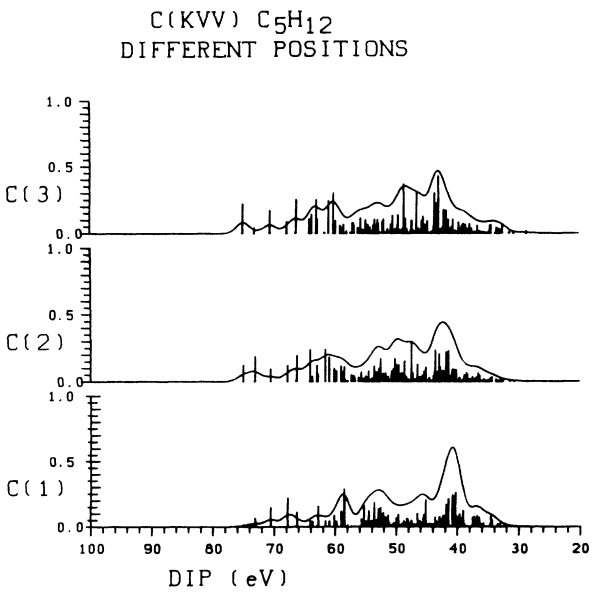

FIG. 6. Carbon Auger spectra for different atoms in C_5H_{12}. Atoms numbered subsequently from end to middle cluster positions.

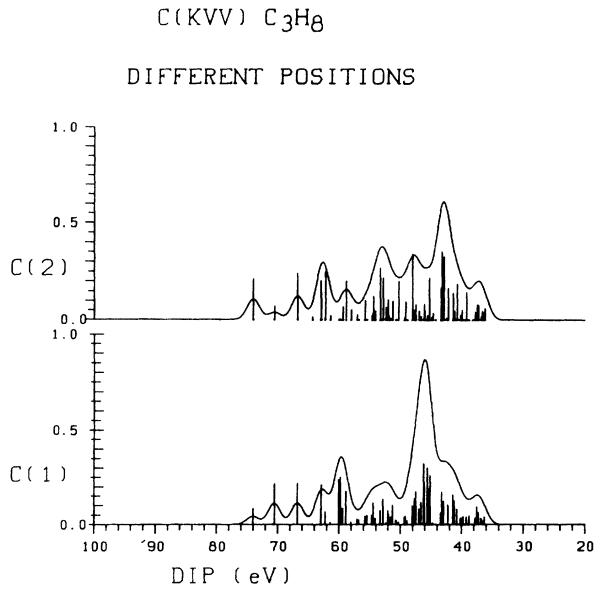

FIG. 8. Carbon Auger spectra for different atoms in C_3H_8. Atoms numbered subsequently from end to middle cluster positions.

limitations and the use of unrenormalized orbital energies in Eq. (4) lead to a systematic overestimation of two-hole binding energies by about 5 eV. Instead of correcting this semiempirically, we kept to considering relative energies only.

III. RESULTS AND DISCUSSION

The resulting spectra are given in Figs. 1–10, where Figs. 1–4 belong to the polyacetylene sequence and Figs. 5–10 to the polyethylene sequence. Tables I and II contain the gross atomic populations and orbital energies for the valence orbitals for both cluster sequences. The trends of the atomic populations for the molecular orbitals together with the distances between the energy levels (determining the density of states) manifest themselves in the Auger spectra.

In the case of the acetylene clusters, Figs. 1–4 show the changes of Auger spectra when going from small to larger systems. Increasing the cluster size the smaller energy spacings between the energy levels produce a smoother spectrum (no pronounced gaps occur between the different DIP regions). This can be seen from the superpositions of the spectra belonging to the nonequivalent carbon atoms (with the corresponding core-level shifts) in Fig. 4.

The influence of the chemical environment on the spectra results in similar spectra for carbon atoms in similar

TABLE I. Gross atomic populations and energies for the valence orbitals of the polyacetylene sequence (energies in eV).

	Orbital no.	Orbital energy	Gross atomic[b] populations			
			c_1			H[a]
C_2H_4	3	−28.57	0.894			0.025
	4	−21.16	0.646			0.048
	5	−16.70	0.658			0.289
	6	−16.23	0.701			0.038
	7	−13.09	0.450			0.437
	8	−12.03	1.000			0.000
			c_1	c_2		H
C_4H_6	5	−30.90	0.303	0.623		0.005
	6	−28.00	0.507	0.403		0.017
	7	−22.79	0.380	0.420		0.046
	8	−21.44	0.209	0.457		0.003
	9	−18.50	0.322	0.405		0.009
	10	−17.50	0.446	0.282		0.085
	11	−15.84	0.307	0.356		0.065
	12	−14.72	0.501	0.043		0.298
	13	−14.22	0.324	0.676		0.000
	14	−13.88	0.369	0.164		0.304
	15	−10.65	0.640	0.360		0.000
			c_1	c_2	c_3	H
C_6H_8	7	−31.54	0.113	0.300	0.528	0.002
	8	−29.93	0.328	0.452	0.151	0.007
	9	−27.78	0.342	0.264	0.311	0.012
	10	−23.82	0.261	0.311	0.291	0.027
	11	−21.77	0.076	0.222	0.380	0.000
	12	−21.42	0.290	0.286	0.114	0.020
	13	−19.03	0.113	0.294	0.467	0.042
	14	−18.69	0.269	0.219	0.273	0.000
	15	−16.83	0.327	0.257	0.144	0.002
	16	−16.52	0.328	0.308	0.047	0.100
	17	−15.56	0.128	0.111	0.363	0.060
	18	−14.90	0.126	0.323	0.551	0.000
	19	−14.90	0.126	0.232	0.551	0.000
	20	−14.09	0.362	0.095	0.093	0.279
	21	−12.91	0.404	0.541	0.055	0.000
	22	−9.96	0.427	0.173	0.400	0.000

[a]Saturating hydrogen atom.
[b]Carbon atoms numbered in increasing order from end to middle cluster positions.

TABLE II. Gross atomic populations and energies for the valence orbitals of the polyethylene sequence (energies in eV).

	Orbital no.	Orbital energy	Gross atomic[a] populations		
			c_1		
CH_4	2	−26.90	1.36		
	3	−16.47	1.17		
	4	−16.47	1.17		
	5	−16.47	1.17		
			c_1		
C_2H_6	3	−26.68	0.72		
	4	−21.94	0.58		
	5	−15.61	0.56		
	6	−15.61	0.56		
	7	−12.61	0.84		
	8	−12.52	0.46		
			c_1		c_2
C_3H_8	4	−30.48	0.47		0.79
	5	−26.64	0.64		0.22
	6	−23.10	0.35		0.59
	7	−18.91	0.34		0.65
	8	−18.12	0.53		0.35
	9	−16.87	0.55		0.35
	10	−16.27	0.59		0.00
	11	−14.91	0.38		0.54
	12	−14.86	0.54		0.41
	13	−14.59	0.23		0.51
			c_1		c_2
C_4H_{10}	5	−30.75	0.24		0.65
	6	−27.62	0.52		0.31
	7	−23.88	0.47		0.24
	8	−22.64	0.19		0.46
	9	−19.21	0.17		0.50
	10	−17.09	0.44		0.18
	11	−16.98	0.23		0.61
	12	−16.57	0.41		0.40
	13	−15.10	0.40		0.14
	14	−14.69	0.34		0.40
	15	−14.38	0.12		0.34
	16	−13.60	0.54		0.02
	17	−12.41	0.42		0.17
			c_1	c_2	c_3
C_5H_{12}	6	−31.21	0.14	0.44	0.62
	7	−28.93	0.38	0.43	0.12
	8	−25.80	0.44	0.17	0.36
	9	−23.04	0.36	0.27	0.09
	10	−22.72	0.11	0.32	0.44
	11	−19.47	0.09	0.34	0.48
	12	−17.86	0.30	0.33	0.00
	13	−17.31	0.13	0.44	0.54
	14	−16.98	0.31	0.32	0.43
	15	−16.00	0.39	0.00	0.38
	16	−14.99	0.20	0.34	0.32
	17	−14.99	0.42	0.36	0.03
	18	−14.67	0.26	0.26	0.00
	19	−14.36	0.07	0.23	0.29
	20	−13.33	0.47	0.03	0.10
	21	−12.44	0.46	0.11	0.21

TABLE II. (*Continued*).

	Orbital no.	Orbital energy	Gross atomic[a] populations		
			c_1	c_2	c_3
C_6H_{14}	7	−31.29	0.08	0.30	0.51
	8	−29.66	0.26	0.45	0.16
	9	−27.21	0.37	0.20	0.26
	10	−24.22	0.36	0.16	0.23
	11	−22.78	0.07	0.23	0.35
	12	−22.69	0.26	0.31	0.09
	13	−19.59	0.06	0.23	0.39
	14	−18.39	0.21	0.36	0.08
	15	−17.39	0.17	0.34	0.34
	16	−17.39	0.14	0.24	0.47
	17	−16.79	0.33	0.08	0.20
	18	−15.48	0.24	0.29	0.26
	19	−15.24	0.33	0.40	0.04
	20	−15.24	0.30	0.05	0.20
	21	−14.42	0.19	0.21	0.32
	22	−14.42	0.17	0.27	0.05
	23	−14.34	0.04	0.16	0.24
	24	−13.06	0.47	0.03	0.05
	25	−12.49	0.38	0.11	0.16

[a]Carbon numbered in increasing order from end to middle cluster positions.

environments. This can be seen from Figs. 1 and 2 by comparing the spectrum of the middle carbon of C_4H_6 with the spectrum of the second carbon in C_6H_8. (The carbon atoms are numbered in increasing order from the end to the middle cluster positions.)

In the theoretical ethylene spectrum there is a gap at $U_{DIP} \simeq 50$ eV which divides the spectrum into a high DIP and a low DIP part. This gap disappears in the middle

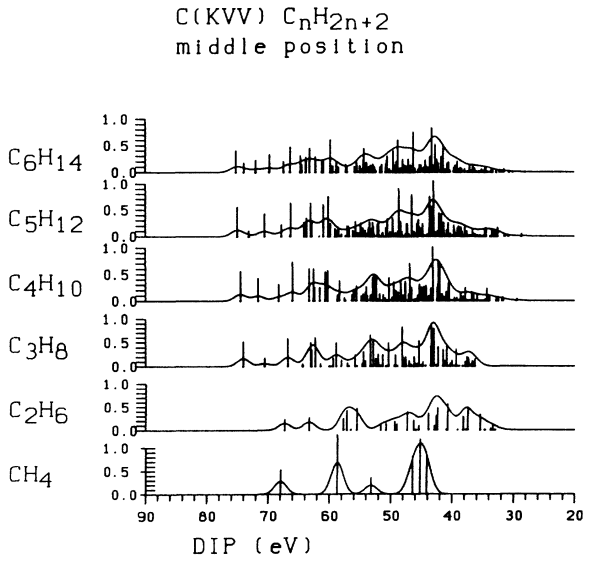

FIG. 9. Middle carbon Auger spectra for different clusters of the polyethylene sequence.

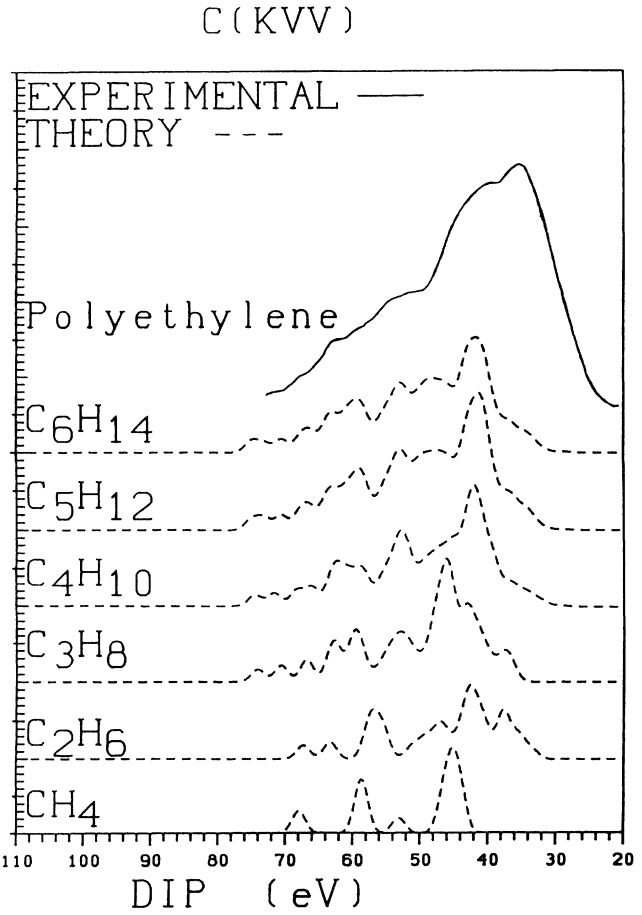

FIG. 10. Comparison of the resulting cluster Auger spectra of the polyethylene sequence with the experimental Auger spectrum of polyethylene from Ref. 4.

carbon spectra of the larger clusters as shown in Fig. 3. For the end atom spectra the gap does not completely disappear.

The main difference between end and middle carbon spectra in the low DIP region (40–50 eV) is a more pronounced peak structure due to the extra hydrogen at the cluster end, which are responsible for a more ethylenelike chemical environment. In the case of C_6H_8 this difference between end and middle carbon spectra is dominated by orbitals 19 and 20, which have a large population at the extra hydrogen atoms and a small population at the carbon atoms in the middle of the cluster.

The more pronounced separation of low and high DIP groups in the case of the end carbon atoms can be explained in a similar way. The end atoms in C_6H_8 have very small populations in orbitals 11 and 13. This has a similar effect for the end atom spectra as omitting orbitals 11 and 13 and thus obtaining a spectrum similar to that of C_2H_4 (large distances between the orbital energy levels manifest themselves in a more separated structure of the Auger spectra).

In Fig. 4 we compared our calculated spectra with the experimental spectra of ethylene and benzene which may serve as an approximate polyacetylene spectrum. In fact, the C_6H_8 spectrum shows the main qualitative features of the benzene spectrum compared to the ethylene spectrum, namely the almost complete disappearance of various gaps which are visible in the ethylene spectrum (mainly that at $U_{\mathrm{DIP}} \approx 48$ eV in the theoretical spectrum which corresponds to the gap at $U_{\mathrm{DIP}} \approx 42$ eV in the experimental spectrum) and the emergence of an additional delocalization shoulder at $U_{\mathrm{DIP}} \approx 30$ eV. This kind of delocalization feature is frequently observed in extended systems and is due to the possibility of two-hole states with the holes localized at different ends of the system. In that case the hole-hole repulsion is very small and the corresponding peak in the spectrum is situated at low DIP values.

The resulting spectra for the ethylene sequence are given in Figs. 5–10. All spectra show features characteristic for sp^3 hybridization, most pronounced in the case of methane, where the low DIP peak belongs to two holes in the degenerate t_2 orbitals while the middle peak is due to a combination of holes in a_1 and t_2 orbitals and the high DIP peak belongs to two holes in the a_1 orbital.

The three-peak structure remains approximately recognizable also for large clusters. The three peaks seem to be dissolved for propane but reappear in smeared out form for pentane, as can be seen by following the sequence of middle carbon spectra given in Fig. 9 going from methane to pentane. The reason is the following: In the limit of infinitely large clusters one has two separate continuous bands, C-C bands with mainly C_{2s} character and C-H bands with mainly C_{2p} and H_{1s} character (although other components are contributing as well[33]). The three-peak structure for larger clusters is due to the three possible combinations of the two band regions.

For the end carbon atoms we get a more pronounced peak structure for the large clusters due to the methyllike chemical environment (Figs. 5–7). This effect can be explained with the help of Table II, where populations at the end carbon atoms are small for some orbitals and, therefore, the orbitals with appreciable populations at these atoms can be divided into two groups, corresponding to the a_1 and t_2 orbitals of methane.

Another important feature is the pronounced high-energy shoulder visible in the end-atom spectrum of propane due to large populations of the high-lying levels at the end carbon atoms. The shoulder disappears in the spectra of the large clusters, where only the usual delocalization peaks occur.

Since the methylene-like environment of the middle carbon atoms is a good model for the polymer polyethylene, it is interesting to see from Fig. 9 that the corresponding cluster spectra converge to the bulk limit even in the case of relatively small clusters. The superpositions of the spectra of the nonequivalent atoms of the various clusters also converge to a limit spectrum which qualitatively reproduces the experimental polyethylene Auger spectrum as shown in Fig. 10.

IV. CONCLUSIONS

Our calculations on the Auger spectra of clusters modeling polyacetylene and polyethylene chains have provided us with a set of comparable *ab initio* results obtained within a consistent set of approximations. The accuracy of the calculations limits the discussion to qualitative changes in the line shape of the spectra. These are, however, now predictable without referring to experimental results.

In the polyacetylene sequence the almost complete disappearance of various gaps, which are visible in the ethylene spectrum, and the emergence of a delocalization feature at $U_{\mathrm{DIP}} \approx 30$ eV is observed. In the polyethylene sequence a three-peak structure, present in methane, is perturbed for propane, but reemerges in broadened form for the large clusters.

ACKNOWLEDGMENTS

Financial support of the Deutsche Forschungsgemeinschaft (Project No. Li 438/1-1) is gratefully acknowledged.

[1]R. R. Rye, T. E. Madey, J. E. Houston, and P-H. Holloway, J. Chem. Phys. **69**, 1504 (1978), and references therein.

[2]R. R. Rye, D. R. Jennison, and J. E. Houston, J. Chem. Phys. **73**, 4867 (1980).

[3]S. W. Gaarenstrom, J. Vac. Sci. Technol. **16**, 600 (1979).

[4]J. A. Kelber, R. R. Rye, G. C. Nelson, and J. E. Houston, Surf. Sci. **116**, 148 (1982).

[5]M. Dayan and S. V. Pepper, Surf. Sci. **138**, 549 (1984).

[6]J. A. Kelber and D. R. Jennison, J. Vac. Sci. Technol. **20**, 848 (1982).

[7]F. L. Hutson and D. E. Ramaker, Phys. Rev. B **35**, 9799 (1987).

[8]I. B. Ortenburger and P. S. Bagus, Phys. Rev. A **11**, 1501 (1975).

[9]K. Faegri, Jr. and R. Manne, Mol. Phys. **31**, 1037 (1976).

[10]I. H. Hillier and J. Kendrick, Mol. Phys. **31**, 849 (1976).
[11]D. R. Jennison, Chem. Phys. Lett. **69**, 435 (1980).
[12]N. Kosugi, T. Ohta, and H. Kuroda, Chem. Phys. **50**, 373 (1980).
[13]O. M. Kvalheim, Chem. Phys. Lett. **86**, 159 (1982).
[14]M. Higashi, E. Hiorike, and T. Nakajima, Chem. Phys. **68**, 377 (1982); **85**, 133 (1984).
[15]D. P. Chong, Chem. Phys. Lett. **82**, 511 (1981).
[16]C.-M. Liegener, Chem. Phys. **92**, 97 (1985); E. Ohrendorf, H. Köppel, L. S. Cederbaum, F. Tarantelli, and A. Sgamellotti, J. Chem. Phys. **91**, 1734 (1989).
[17]F. Tarantelli, A. Sgamellotti, L. S. Cederbaum, and J. Schirmer, J. Chem. Phys. **86**, 2201 (1987).
[18]K. Siegbahn, C. Nordling, G. Johansson, J. Hedman, P. F. Heden, K. Hamrin, U. Gelius, T. Bergmark, L. O. Werme, R. Manne, and Y. Baer, *ESCA Applied to Free Molecules* (North-Holland, Amsterdam, 1969).
[19]J. W. Rogers, Jr., H. C. Peebles, R. R. Rye, J. E. Houston, and J. S. Binkley, J. Chem. Phys. **80**, 4513 (1984).
[20]O. M. Kvalheim, Chem. Phys. Lett. **98**, 457 (1983).
[21]N. Correia, A. Flores-Riveros, H. Ågren, K. Helenelund, L. Asplund, and U. Gelius, J. Chem. Phys. **83**, 2035 (1985).
[22]C.-M. Liegener, Chem. Phys. Lett. **90**, 188 (1982); Phys. Rev. A **28**, 256 (1983); J. Chem. Phys. **79**, 2924 (1983); J. Phys. B **16**, 4281 (1983); Chem. Phys. Lett. **106**, 201 (1984); **123**, 92 (1986).
[23]J. Schirmer and A. Barth, Z. Phys. A **317**, 267 (1984); F. Tarantelli, A. Tarantelli, A. Sgamellotti, J. Schirmer, and L. S. Cederbaum, J. Chem. Phys. **83**, 4683 (1985); F. Tarantelli, A. Tarantelli, A. Sgamellotti, J. Schirmer, and L. S. Cederbaum, Chem. Phys. Lett. **177**, 577 (1985); F. Tarantelli, J. Schirmer, A. Sgamellotti, and L. S. Cederbaum, *ibid.* **122**, 169 (1985).
[24]D. Sinha, S. K. Mukhopadhyay, M. D. Prasad, and D. Mukherjee, Chem. Phys. Lett. **125**, 213 (1986).
[25]C.-M. Liegener, A. K. Bakhshi, R. Chen, and J. Ladik, J. Chem. Phys. **86**, 6039 (1987).
[26]J.A.D. Matthew and Y. Komninos, Surf. Sci. **53**, 716 (1973).
[27]H. Siegbahn, L. Asplund, and P. Kelfve, Chem. Phys. Lett. **35**, 330 (1975).
[28]E. J. McGuire, Phys. Rev. **185**, 1 (1969).
[29]L. Gianolio, R. Pavani, and E. Clementi, Gazz. Chim. Ital. **108**, 181 (1978).
[30]*Tables of Interatomic Distances in Molecules and Ions,* edited by L. E. Sutton, D. G. Jenkin, A. D. Mitchell, and L. C. Cross (Chemical Society, London 1958/1965).
[31]F. L. Hutson and D. E. Ramaker, J. Chem. Phys. **87**, 6824 (1987).
[32]D. E. Ramaker, in *Chemistry and Physics of Solid Surfaces IV,* edited by R. Vanselow and R. Howe (Springer, Berlin, 1982), p. 19.
[33]J. Delhalle, J.-M. André, S. Delhalle, J. J. Pireaux, R. Caudano, and J. J. Verbist, J. Chem. Phys. **60**, 595 (1974).